Nanoscale Res Lett (2010) 5:1846–1851
DOI 10.1007/s11671-010-9726-7

NANO EXPRESS

Preparation and Characterization of Silica/Polyamide-imide Nanocomposite Thin Films

Xiaokun Ma · Nam-Hee Lee · Hyo-Jin Oh · Jong-Sun Hwang · Sun-Jae Kim

Received: 28 June 2010 / Accepted: 26 July 2010 / Published online: 7 August 2010

Abstract The functional silica/polyamide-imide composite films were prepared via simple ultrasonic blending, after the silica nanoparticles were modified by cationic surfactant—cetyltrimethyl ammonium bromide (CTAB). The composite films were characterized by scanning electron microscope (SEM), thermo gravimetric analysis (TGA) and thermomechanical analysis (TMA). CTAB-modified silica nanoparticles were well dispersed in the polyamide-imide matrix, and the amount of silica nanoparticles to PAI was investigated to be from 2 to 10 wt%. Especially, the coefficients of thermal expansion (CET) continuously decreased with the amount of silica particles increasing. The high thermal stability and low coefficient of thermal expansion showed that the nanocomposite films can be widely used in the enamel wire industry.

Keywords Composites · Fracture · Surfaces · Thermal properties · Thin films

Introduction

Polyamide-imide (PAI) is a kind of thermoplastic resin, has good high-temperature resistance, outstanding mechanical properties and excellent oxidative stability, all of which have led PAI to have been widely used with electronic materials, adhesives, composite materials, fiber, and film material [1–8]. Comparing with the polyimide and polyamide, the PAI own the better process ability and heat-resistant properties. The basic studies of the synthesized PAI have attracted increasing interest for a wire-coating material with a thermal resistant property. However, an increasing number of breakdown cases have been reported when a higher surge voltage exists in some devices. Therefore, the development of an inorganic/organic nanocomposite insulating material should be widely discussed to improve the electrical life of enameled wires [9–11].

Actually, there are so many factors affecting the properties of hybrid composites, such as the particle size, size distribution, and filler content. In addition, the inorganic particle shape, surface structure, and mechanical properties of a filler (stiffness, strength, etc.) all play an important role in the synthesizing of inorganic/organic composite materials. Especially, the bond strength between inorganic particles and polymer matrix should be improved, which always was influenced by the type of dispersion aid or coupling agent used [12–18].

Silica nanoparticles as a very important inorganic material have emerged as an area of intense current interest motivated because of their special physical and chemical properties, such as their small size, strong surface energy, high scattered performance, and thermal resistance [19–23]. However, the applications of silica nanoparticles are largely limited because of their high energetic hydrophilic surface, which causes the silica nanoparticles to be easily agglomerated. Fortunately, this problem could be resolved by using some surface modification methods with different surfactant agents. In other words, the strong interface adhesion between the organic matrix and silica nanoparticles is a key to the application of silica nanoparticles as fillers.

X. Ma · N.-H. Lee · H.-J. Oh · S.-J. Kim (✉)
Institute/Faculty of Nanotechnology and Advanced Materials Engineering, Sejong University, #98 Gunja-dong, Gwangjin-gu, Seoul 143-747, South Korea
e-mail: sjkim1@sejong.ac.kr

J.-S. Hwang
Department of Computer Applied Electricity, Jeonnam Provincial College, #262 Hyangyo-Ri, Damyang-Eup, Damyang-Gun, Jeonnam 517-802, South Korea

Jadav et al. [24] had successfully synthesized the silica/polyamide nanocomposite film via interfacial polymerization process using two types of silica nanoparticles of size about 16 and 3 nm, respectively. The nanocomposite films exhibit superior thermal stability than the pure polyamide membranes. In this work, the authors observed that silica nanoparticles loading could significantly modify the polyamide network structure, pore structure and transport properties. The excellent membrane performance in terms of separation efficiency and productivity flux was discussed. Zhang et al. [25] prepared a novel isometric polyimide/silica hydrid material through sol–gel technique. At the beginning, 3-[(4-phenylethynyl) phthalimide]propyl triethoxysilane (PEIPTES) was synthesized to be used for modifying nano-silica precursor. Then the isomeric polyimide/silica hybrid material was produced by using isomeric polyimide resin solution and the modified nano-silica precursor after heat treatment process. The isomeric polyimide/silica composite has much better thermal properties and nano-indenter properties than those of isomeric polyimide.

In this work, cationic surfactant CTAB was chosen to modify the silica nanoparticles and the amount of CTAB to silica nanoparticles was changed from 0 to 3 wt%. After the surface modification process, the CTAB-modified silica nanoparticles had the better compatibility with PAI polymer matrix and the CTAB-modified silica nanoparticles could be well dispersed into the PAI matrix, even when the amount of silica to PAI reached to 10 wt%. The thermal properties were obviously improved, and the decomposition temperature was increased with the amount of silica increasing.

Experiment

Materials

Silica nanoparticles were purchased from Sigma–Aldrich Company, and the size of the nano-silica was 10–20 nm. Commercial polyamide-imide powder (PAI, Torlon AI-10) was purchased from Solvay Company (USA). Cetyltrimethyl Ammonium Bromide (C16, CTAB, 99% purity, ACROS) was used as a surface modification agent. *N*,*N*-Dimethylformamide (DMF) was anhydrous and was purchased from Sigma–Aldrich Company. Sodium hydroxide (NaOH) was purchased from Sam Chun Co (Korea). Ethanol was a chemical reagent and was purchased from DUKSAN Pure Chemicals. Distilled and deionized water was used throughout the work.

Bar coater 08, coating rods are used primarily to apply a variety of coatings or emulsions to a multitude of substrates. Stainless steel rods are wrapped very tightly with stainless steel wire and the diameter of wire are 0.2 mm. In this work, the silica/PAI composite films were cast by bar coater to make the films more uniform.

Preparation and Surface Modification of Silica Nanoparticles

In a typical experiment, 100 ml deionized water and 1.000 g silica particles were added to the flask, and the solution was adjusted to pH 8 by the addition of 0.1 M NaOH. Then the silica nanoparticles were modified at 65°C under constant stirring with CTAB added into the system. In order to improve the dispersal state of the silica nanoparticles in the PAI matrix, the amount of CTAB to silica nanoparticles was changed from 0 to 3.0 wt%. After the surface modification process, the modified nano-silica particles were collected by suction filtration and then dried at 90°C for 6 h.

Preparation of Silica/Polyamide-imide Nanocomposite Films

The silica/PAI nanocomposite films were prepared through the simple ultrasonic blending. *N*,*N*-dimethyl form amide (DMF) was used as a solvent and 2.0 g of PAI powder were dissolved in 3 ml of DMF. The silica nanoparticles were added into the solution, the amount of silica to PAI was changed from 2 to 10 wt%. The mixture was ultrasonic dispersed $\sim$3 h at room temperature. In the next step, the mixture solution was cast on a square glass plate (5*5 cm) by the bar coater. The films were initially heated to remove the solvent in the vacuum oven and the temperature was controlled as follows: at 60°C for 4 h, at 80°C for 2 h, then raised to 120°C for 1 h; finally, the films were heated at 160°C for 1 h. The experiment details of the process of silica/PAI composite films are shown in Scheme 1.

Characterization

The fracture surface of composites films were determined by a Hitachi Co. S-4700 scanning electron microscope (SEM). Before SEM imaging, the samples were sputtered with thin layers of Pt–Pd. A Scinco STA S-1500 simultaneous thermal analyzer was applied to analyze the thermal stability of the nano-silica/PAI composite films. The samples were heated from 30 to 800°C at 10°C/min in an air atmosphere. The coefficients of thermal expansion (CET) of silica/PAI composites films were evaluated by a Q 400 EM (USA) thermomechanical analysis (TMA) (5°C/min from 25 to 300°C, 50 mN). All the samples were of 3 × 16 mm, which were cut from original films using a razor blade.

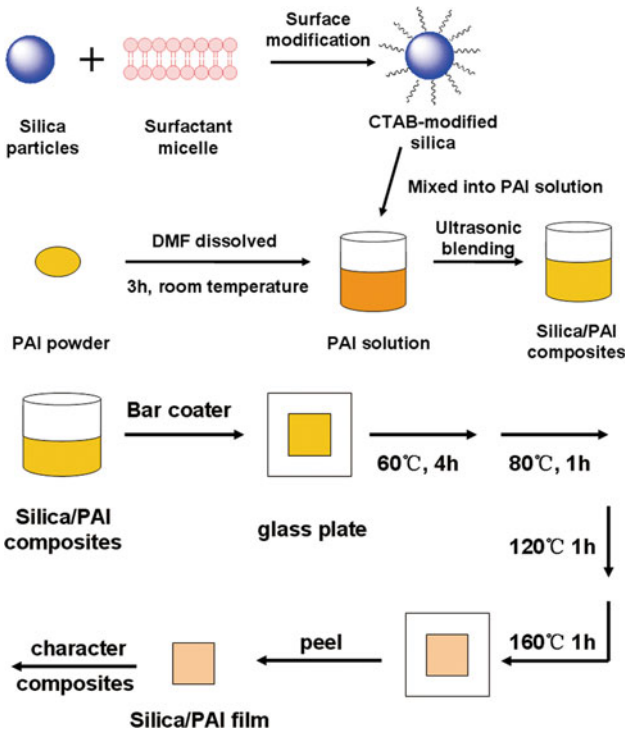

Scheme 1 Preparation process of the silica/PAI nanocomposite films

Results and Discussion

FT-IR Spectra of the Silica/PAI Composite Films

The FT-IR spectra of silica/PAI composite films were shown in Fig. 1. In order to compare the effect of surfactant on composite films, the amount of silica nanoparticles to PAI was all 6 wt%, while the dosage of CTAB to silica was changed from 0 to 3 wt%. The character vibrations of Si–O were found at 1,086, 945 and 796 cm^{-1}, as shown in Fig. 1e. After the surface modification process, the typical stretching vibrations of the C–H were found at 2,855 and 2,928 cm^{-1}, which results from the $–CH_2$ and $–CH_3$ in the CTAB. As shown in Fig. 1, the typical characteristic bands of PAI polymer matrix were found. Such as the N–H stretching band at 3,317 cm^{-1}, amide C=O region around 1,710 cm^{-1} and the bands at 1,771 and 1,710 cm^{-1} are associated with the imide carbonyl band. These bands were similar with each other due to the same amount of silica added into the composites. It was worth pointing out that the characteristic stretching vibration of Si–O at 1,086 cm^{-1} became wider, when the silica nanoparticles were modified by CTAB. It could be explained that the organic chain-side of CTAB were grafted on the surface of silica nanoparticles, which made the interaction between the silica nanoparticles and PAI polymer matrix had been improved.

Then, the amount of silica to PAI was changed from 2 to 10 wt% and the dosage of CTAB to silica was at 3 wt%, the FT-IR spectra of pure PAI and some silica/PAI composite films were shown in Fig. 2. In those spectra, the bands at 1,771 and 1,710 cm^{-1} were associated with the imide carbonyl band and they were so insensitive to the presence of the silica nanoparticles. The bands in the region from 945 to 650 cm^{-1} increased with the silica content increasing, due to the presence of a broad band associated with the vibration of Si–O band. On the other hands, the N–H stretching band at 3,317 cm^{-1} increased slightly in intensity with the silica content increasing, suggesting hydrogen-bonded N–H groups in the PAI polymer and the Si–O–Si or Si–O–H groups of the silica nanoparticles. The characteristic band at 1,594 cm^{-1} came

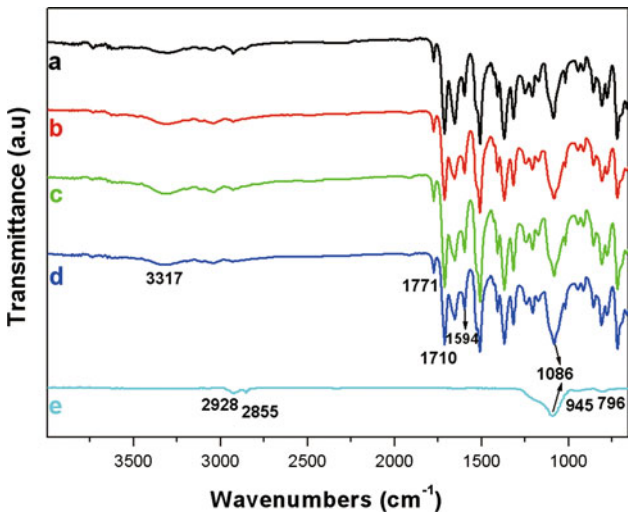

Fig. 1 FT-IR spectra of **a** unmodified-silica/PAI composites; **b** 1.0 wt%CTAB-silica/PAI composites; **c** 2.0 wt%CTAB-silica/PAI composites; **d** 3.0 wt%CTAB-silica/PAI composites; **e** CTAB-modified silica nanoparticles

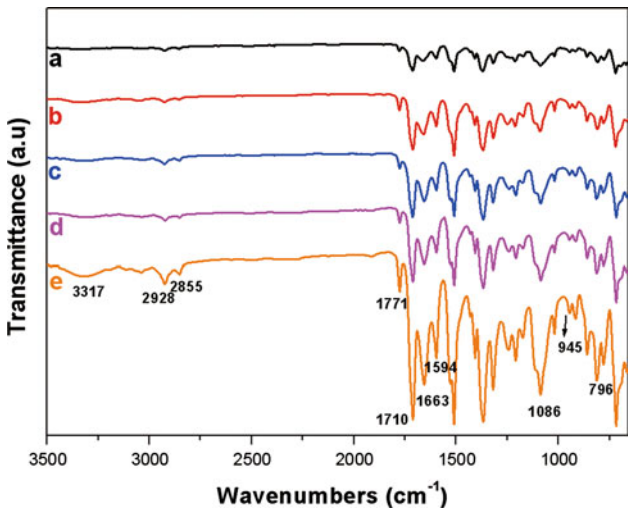

Fig. 2 FT-IR spectra of silica/PAI composite with the amount of silica to PAI **a** 2 wt%; **b** 4 wt%; **c** 6 wt%; **d** 8 wt%; **e** 10 wt%

from the benzene ring stretch and a contribution from O–H bonding in monomeric water, which also has a band at 1,663 cm^{-1}. In conclusion, all the characteristic peaks in the composites indicated that the interaction between the silica nanoparticles and PAI polymer matrix were sensitive to the amount of silica in composites.

SEM Micrographs of Silica/PAI Composite Films Fracture Surface

The fracture surface micrographs of silica/PAI composite films are shown in Fig. 3. In Fig. 3a, some silica agglomerations could be found in the micrograph, when the unmodified-silica nanoparticles were added into the PAI matrix. As we knew, silica nanoparticles were easy to agglomerate together; however, the CTAB-modified silica nanoparticles could be dispersed well in the PAI matrix with the amount of CTAB increasing. The dispersal state of the silica nanoparticles was improved when the silica nanoparticles were modified with 1wt % CTAB, as shown in Fig. 3b. In Fig. 3c, the silica nanoparticles were almost monodispersed and a little agglomeration could be found, when 2 wt% CTAB modified silica nanoparticles were added into the PAI polymer. Especially, after the silica were modified with 3 wt% CTAB, the silica nanoparticles became monodispersed without any agglomerations even though the amount of silica nanoparticles to PAI increased to 6 wt%, as shown in Fig. 3d. As a result, the CTAB could improve the dispersal state of silica nanoparticles in a PAI polymer matrix and the optimal dosage of CTAB to silica nanoparticles was 3 wt%.

The fractured surfaces micrographs of pure PAI and several composite films are shown in Fig. 4. First of all, the fracture surfaces of pure PAI film were uniform and the continuous polymer phase is shown in Fig. 4a. Figure 4b–f shows the fracture surface of different silica/PAI composites, and the amount of silica to PAI changed from 2 to 10 wt%. The more silica nanoparticles were added into PAI, the more of them that could be found in the fracture surface micrographs. In Fig. 4f, when the 10 wt% silica nanoparticles were added into PAI, the silica nanoparticles still were monodispersed without any agglomerations. The results indicated that the CTAB-modified silica nanoparticles had the better dispersal state in the PAI polymer matrix and could increase the content of silica nanoparticles in composites. The surface modification process is an effective method to prepare the silica/PAI nanocomposite.

Thermal Stability of Silica/PAI Composite Films

The thermal stability of silica/PAI composite films was evaluated by thermogravimetric analysis. TGA plots of PAI and composites with the different amounts of silica nanoparticles were shown in Fig. 5. The amount of silica nanoparticles to PAI polymer matrix was changed from 0 to 10 wt% and the plots were listed in Fig. 5a–f,

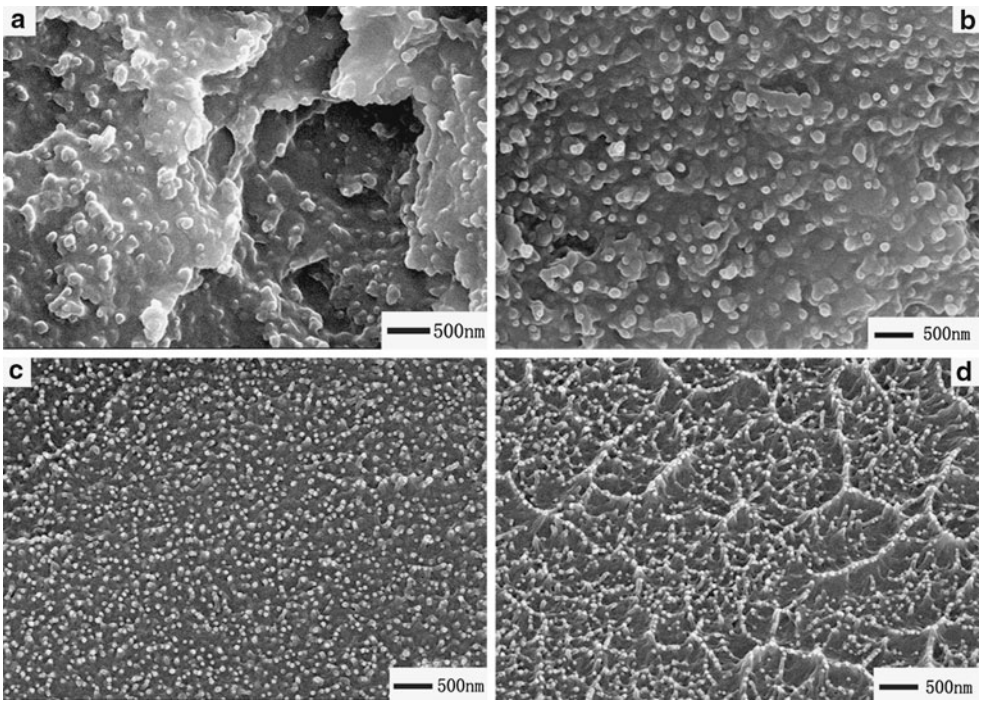

Fig. 3 Fracture surface micrographs of **a** unmodified-silica/PAI composites; **b** 1.0 wt%CTAB-silica/PAI composites; **c** 2.0 wt%CTAB-silica/PAI composites; **d** 3.0 wt%CTAB-silica/PAI composites

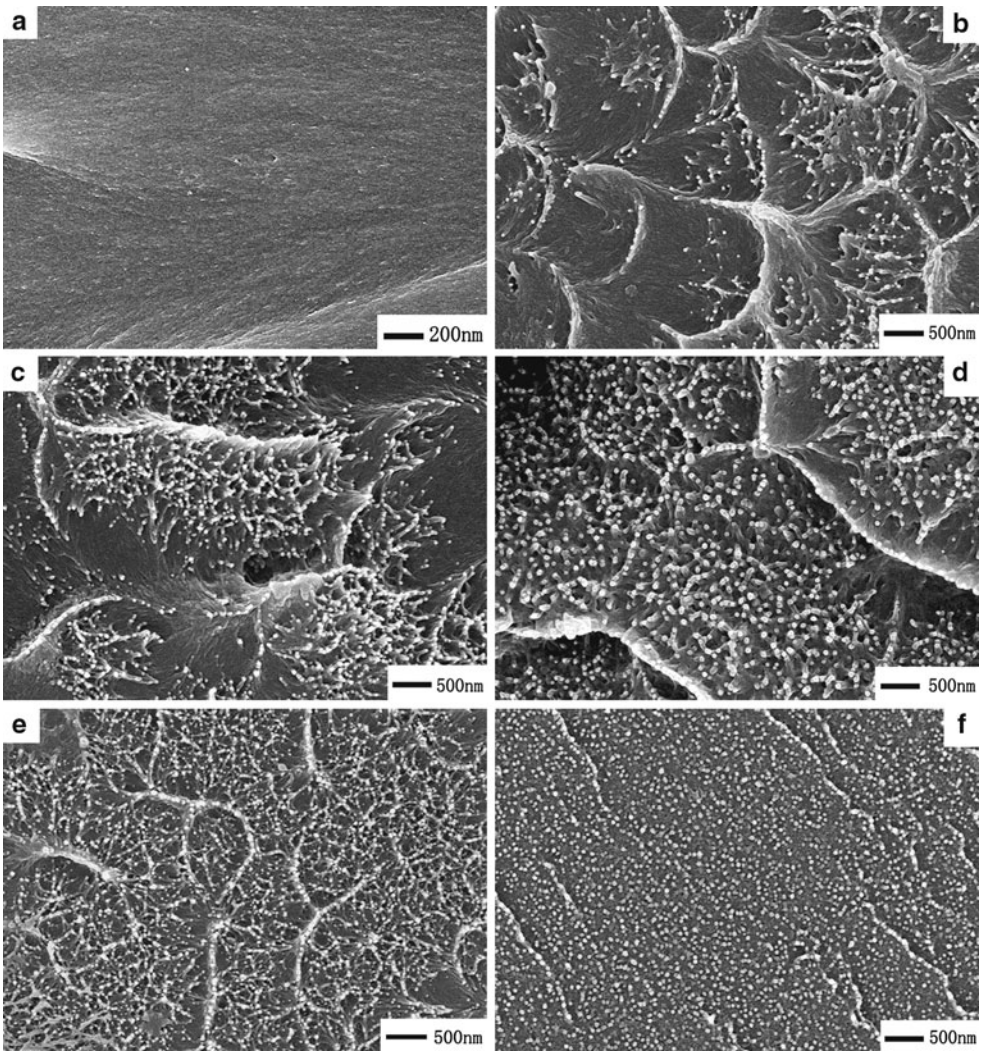

Fig. 4 Fracture surface micrographs of **a** pure PAI and silica/PAI nanocomposite with the amount of silica to PAI, **b** 2 wt%, **c** 4 wt%, **d** 6 wt%, **e** 8 wt%, **f** 10 wt%

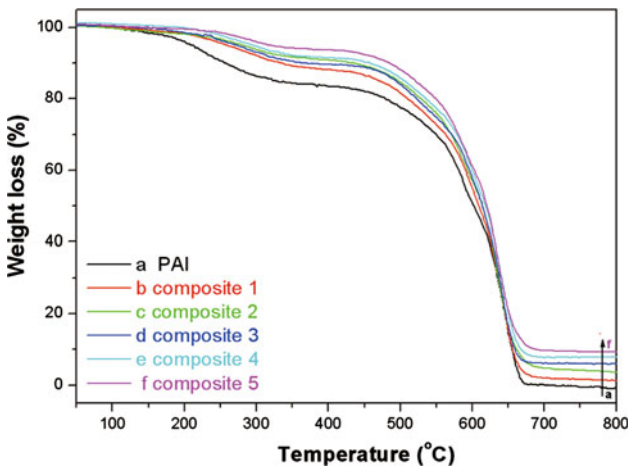

Fig. 5 TGA plots of the PAI matrix (**a**) and silica/PAI nanocomposite films with the amount of silica to PAI (**b**) 2 wt%, **c** 4 wt%, **d** 6 wt%, **e** 8 wt%, **f** 10 wt%

respectively. A weight loss is observed above 170°C on all the TGA plots, which corresponds to the loss of water and solvent. When the temperature was raised to 450°C, the PAI matrix began to decompose and the decomposition temperature became higher when the silica nanoparticles were added into the PAI polymer matrix. At the same temperature, all the curves of the composites indicated that the weight loss of the composites was less than that of the pure PAI matrix. In other words, the silica/PAI composites have a higher decomposition temperature when the PAI polymer matrix loses the same weight. It is worth pointing out that the thermal stability of PAI was enhanced with the increasing silica contents. In addition, the amount of silica nanoparticles in the composites could be calculated accurately in the TGA plots. Figure 5b–f shows that the amounts of silica in composites were 1.9, 3.6, 5.8, 7.3 and 10.2 wt%, respectively.

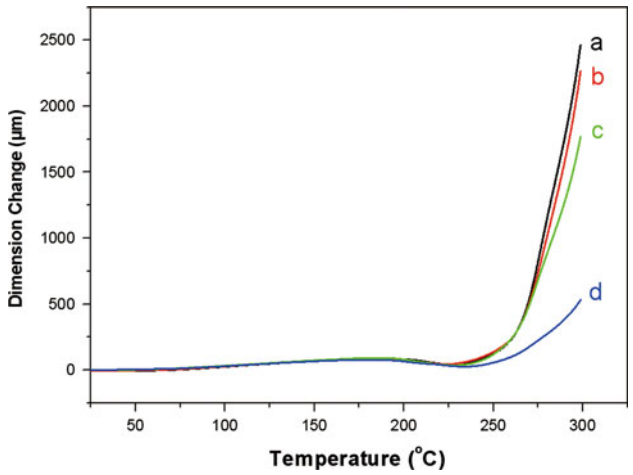

Fig. 6 The CTE curves of the **a** pure PAI film; **b** composite films with 4 wt% silica, **c** composite films with 6 wt% silica; **d** composite films with 10 wt% silica

Coefficient of Thermal Expansion (CTE) of Silica/PAI Composite Films

The coefficient of thermal expansion (CTE) is an important parameter to evaluate the properties of enameled wire. The low CTE could reduce thermal stress build-up and avoid device failure through peeling and cracking at the interface between the polymer film and copper. The CTE curves of pure PAI film and some composite films were shown in Fig. 6. The CTE value of PAI films was 3.87×10^{-5} m/m °C, while the CTE value of silica/PAI composite film was decreased to 3.69×10^{-5} m/m °C and 3.51×10^{-5} m/m °C, when the amount of silica to PAI was 4 and 6 wt%, respectively. The CTE values continuously decreased with the amount of silica particles increasing, especially, the CTE value decreased to 3.35×10^{-5} m/m °C when the amount of silica to PAI was 10 wt%, as shown in Fig. 6d. Compared with PAI polymer film, the silica/PAI composite films had the lower coefficient of thermal expansion (CTE), due to the rigidity and stiffness of silica nanoparticles and the interaction between the silica and PAI polymer matrix. In conclusion, the rigidity and stiffness of silica nanoparticles limited the movement of the polymer chain, which made the thermal expansion of PAI matrix decrease.

Conclusion

The silica/PAI inorganic/organic nanocomposite films were successfully synthesized by the simple ultrasonic blending, after the silica nanoparticles were modified by CTAB. In the fracture surface micrographs of composite films, the silica nanoparticles were found well dispersed in the PAI polymer matrix. The silica nanoparticles were still monodispersed without any agglomerations when the amount of silica nanoparticles to PAI reached 10 wt%. The thermal stability of PAI was improved, and the decomposition temperature was increased when the amount of silica nanoparticles was increased. The lower coefficient of thermal expansion of composite films could reduce the peeling and cracking at the interface between the polymer film and copper. In this system, the high thermal stability and low coefficient of thermal expansion showed that the silica/PAI nanocomposite films can be widely used in the enamel wire industry.

References

1. D. Liaw, P. Hsu, B. Liaw, J. Polym. Sci. Pol. Chem. **39**, 63 (2001)
2. K. Babooram, B. Francis, R. Bissessur, R. Narain, Compos. Sci. Technol. **68**, 617 (2008)
3. D. Liaw, B. Liaw, Polymer **42**, 839 (2001)
4. S. Hsiao, C. Yang, Polym. Sci. Pol. Chem. **28**, 1149 (1990)
5. D. Liaw, W. Chen, Polym. Degrad. Stabil. **91**, 1731 (2006)
6. M. Barikani, S.M. Ataei, J. Polym. Sci. Pol. Chem. **37**, 2245 (1999)
7. Y. Wang, S. Goh, T. Chung, P. Na, J. Membrane Sci. **326**, 222 (2009)
8. G. Entura, E. Gottardi, I. Peroni, A. Peruzzi, G. Ponti, Nucl. Phys.B **78**, 571 (1999)
9. L.W. Chen, K.S. Ho, J. Polym. Sci. Pol. Chem. **35**, 1711 (1997)
10. A. Ranade, N. Souza, B. Gnade, Polymer **43**, 3759 (2002)
11. H. Kikuchi, Y. Yukimon, S. Itonaga, Hitachi Cable Rev. **21**, 55 (2002)
12. K. Kusakabe, K. Ichiki, J. Hayashi, H. Maeda, S. Morooka, J. Membrane Sci. **115**, 65 (1996)
13. S.S. Hossein, Y. Lia, T.S. Chunga, Y. Liu, J. Membrane Sci. **302**, 207 (2007)
14. M. Castellano, L. Conzatti, G. Costa, L. Falqui, A. Turturro, B. Valenti, F. Negroni, Polymer **46**, 695 (2005)
15. M. Alexandre, P. Dubois, Mat. Sci. Eng. R **28**, 1 (2000)
16. I.A. David, G.W. Scherer, Chem. Mater. **7**, 1957 (1995)
17. Y. Yang, P. Wang, Polymer **47**, 2683 (2006)
18. M.D. Butterworth, R. Corradi, J. Johal, S.F. Lascelles, S. Maeda, S.P. Armes, J. Colloid Interf. Sci. **174**, 510 (1995)
19. Y. Ouabbas, A. Chamayou, L. Galet, M. Baron, G. Thomas, P. Grosseau, B. Guilhot, Powder Technol. **190**, 200 (2009)
20. Y.L. Lee, Z.C. Du, W.X. Lin, Y.M. Yang, J. Colloid Interf. Sci. **296**, 233 (2006)
21. S.D. Bhagat, Y.H. Kim, K.H. Suh, Y.S. Ahn, J.G. Yeo, J.H. Han, Micropor. Mesopor. Mater. **112**, 504 (2008)
22. C. Oh, Y.G. Lee, C.U. Jon, S.G. Oh, Colloid. Surf. A **337**, 208 (2009)
23. L. Xue, J. Li, J. Fu, Y. Han, Colloid. Surf. A **338**, 15 (2009)
24. G.L. Jadav, P.S. Singh, J. Membrane Sci. **328**, 257 (2009)
25. C. Zhang, M. Zhang, H. Cao, Z. Zhang, Z. Wang, L. Gao, M. Ding, Compos. Sci. Technol. **67**, 380 (2007)